Quantum oscillations in the parent pnictide $BaFe_2As_2$: Itinerant electrons in the reconstructed state

James G. Analytis,[1,2] Ross D. McDonald,[3] Jiun-Haw Chu,[1,2] Scott C. Riggs,[3] Alimamy F. Bangura,[4] Chris Kucharczyk,[1,2] Michelle Johannes,[5] and I. R. Fisher[1,2]

[1]*Geballe Laboratory for Advanced Materials and Department of Applied Physics, Stanford University, Stanford, California 94305, USA*

[2]*Stanford Institute for Materials and Energy Sciences, SLAC National Accelerator Laboratory, 2575 Sand Hill Road, Menlo Park, California 94025, USA*

[3]*Los Alamos National Laboratory, Los Alamos, New Mexico 87545, USA*

[4]*H. H. Wills Physics Laboratory, University of Bristol, 1 Tyndall Avenue, Bristol BS8 1TL, United Kingdom*

[5]*Center for Computational Materials Science, Code 6390, Naval Research Laboratory, Washington, DC 20375, USA*

(Received 6 February 2009; revised manuscript received 14 July 2009; published 11 August 2009)

We report quantum-oscillation measurements that enable the direct observation of the Fermi surface of the low-temperature ground state of $BaFe_2As_2$. From these measurements we characterize the low-energy excitations, revealing that the Fermi surface is reconstructed in the antiferromagnetic state, but leaving itinerant electrons in its wake. The present measurements are consistent with a conventional band folding picture of the antiferromagnetic ground state, placing important limits on the topology and size of the Fermi surface.

DOI: 10.1103/PhysRevB.80.064507 PACS number(s): 71.18.+y, 74.25.Dw, 75.10.Lp, 75.30.−m

The low-energy quasiparticle dynamics are an essential ingredient to many theories of superconductivity. The Fe-pnictide superconductors however, show evidence for electron itinerancy[1–4] and local magnetism,[5–8] making it difficult to know which theoretical framework is most appropriate for understanding these compounds.[9] Establishing the nature of the itinerancy and magnetism in the parent compounds is therefore of fundamental importance. In the present paper we report quantum oscillation (QO) measurements in $BaFe_2As_2$, consistent with density-functional calculations of the antiferromagnetic ground state. We find that the spin-density wave instability does not fully gap the Fermi surface (just as recently predicted[10]) and quasiparticle coherence persists in the magnetically ordered ground state.

In the measurements reported here on $BaFe_2As_2$ we use two separate techniques, torque magnetometry and a radio-frequency contactless conductivity technique using a tunnel diode oscillator (TDO), both of which have been used recently to observe oscillations in the closely related compounds LaFePO (Ref. 1) and $SrFe_2As_2$.[2] We observe three small pockets comprising 1.7%, 0.7%, and 0.3%, of the paramagnetic Brillouin zone (that associated with the tetragonal state) and produce band-structure calculations of a reconstructed state which are in broad agreement. Furthermore we map the topology of these small pockets and extract their effective mass. The present measurements illustrate that itinerant electrons play a fundamental role in the ordered state of ternary Fe pnictides and place important limits on the topology and size of the Fermi surface in the antiferromagnetic state.

Single crystal samples of $BaFe_2As_2$ were prepared by slow cooling a ternary melt, as described elsewhere.[11,12] The crystals were then annealed at high temperature ~900 °C in vacuum for 24 h to allow interstitial and vacancy disorder to relax. Sample surfaces often appeared degraded after the annealing process but residual resistivity ratios increased from 4 to 10. For these crystals the absolute values of the in-plane resistivity are around ~0.7 mΩ cm at 300 K. Magnetic QO measurements were performed at the National High Magnetic Field Laboratory (Los Alamos) in the short pulse (~10 ms rise time) 65 T and long pulse (~1 s rise time) 60 T magnets. For the torque magnetometry experiments, piezoresistive microcantilevers were used at temperatures down to 0.4 K. The measured torque signal is dependent on the anisotropic magnetization of the sample $\tau \propto \mu_0 \mathbf{M} \times \mathbf{H}$, and can thus detect magnetic field dependent oscillations in the magnetization, known as the Haas-van Alphen effect. Sample A, used on the torque cantilever was $0.2 \times 0.2 \times 0.08$ mm^3. Another sample (sample B) of dimensions $2 \times 2 \times 0.3$ mm^3 was mounted with its tetragonal c axis parallel to the axis of a compensated coil that forms part of the tunnel diode oscillator circuit. The oscillator resonates at frequency ~37 MHz in the absence of an applied field, dropping by ~300 kHz at 65 T in response to the magnetoconductivity of the sample. As the skin depth changes due to the Shubnikov-de Haas effect, the coil-resonance frequency is correspondingly altered.

Background subtracted data taken from sample A is shown in the inset of Fig. 1(a) (a smooth polynomial of order 3). The Fourier content of the data is shown in Fig. 1(a), illustrating the predominance of a single frequency $F_\gamma = 80$ (herein the γ pocket, which appears at 95 T in Fig. 1 because the angle between the field and the tetragonal c axis $\theta = 27°$). In sample B two higher frequencies $F_\alpha = 440$ and $F_\beta = 190$ T appear at $\theta = 0°$ which we shall call the α and β pockets, respectively. The α, β, and γ orbits comprise about 1.7%, 0.7%, and 0.3% of the paramagnetic Brillouin zone.

We extract the effective mass by fitting the temperature dependence of the oscillation amplitude with the thermal damping term $R_T = X/\sinh(X)$ of the Lifshitz-Kosevich (LK) formalism, where $X = 14.69\ m^* T/B$ and m^* is the effective mass. Presently $1/B$ is the average inverse field of the Fourier window, taken between 20 and 60 T.[13] The suppression of the α, β, and γ frequency amplitudes is shown in Fig. 1(b). Data for the γ pocket are shown for both techniques. The effective mass is $m^*_\gamma = 0.9 \pm 0.1 m_e$ in sample A and m^*_γ

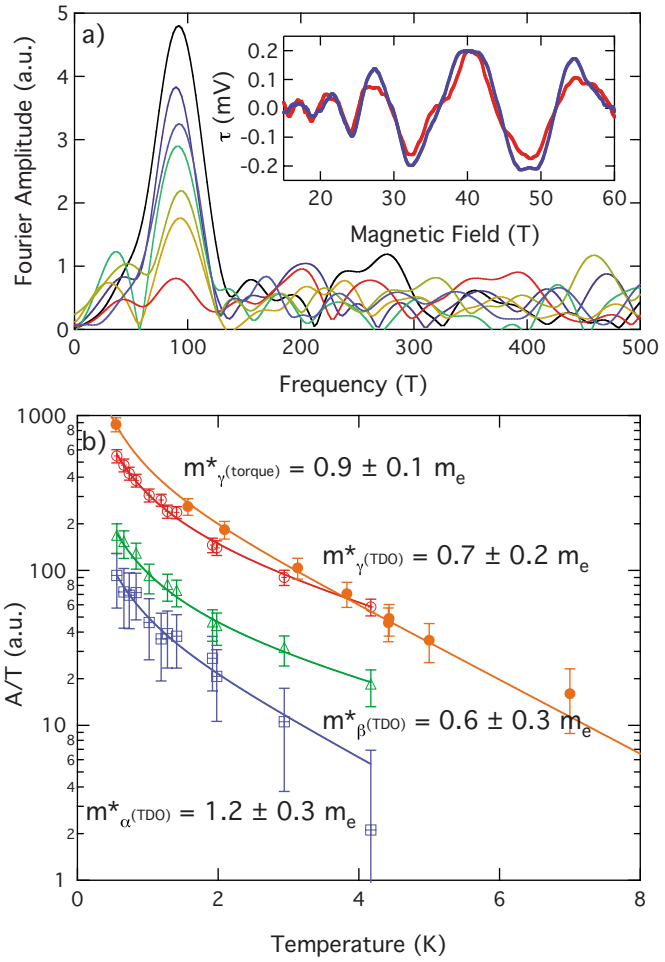

FIG. 1. (Color online) (a) Thermal evolution of the Fourier spectrum of the torque data measured with the applied magnetic field oriented 27° from the c axis. The corresponding temperatures from highest to lowest intensity are 0.5, 2, 3.1, 4.0, 6.0, 8.0, and 9.0 K. The inset shows typical low-temperature (0.5 and 1.5 K) torque data (with background subtracted). (b) The temperature dependence of the Fourier amplitude (a) for the α pocket (open squares), the β pocket (open triangles), the γ pocket (open circles) all measured by the TDO technique, and the γ pocket as measured by torque magnetometry (solid circles). The solid lines are fits to the LK formula yielding the following effective masses: (at $\theta=23°$); $m^{\star}_{\alpha}$(TDO) $=1.2\pm0.3m_e$, $m^{\star}_{\beta}$(TDO)$=0.6\pm0.3m_e$, $m^{\star}_{\gamma}$(TDO)$=0.7\pm0.2m_e$, and $m^{\star}_{\gamma}$(Torque)$=0.9\pm0.1m_e$.

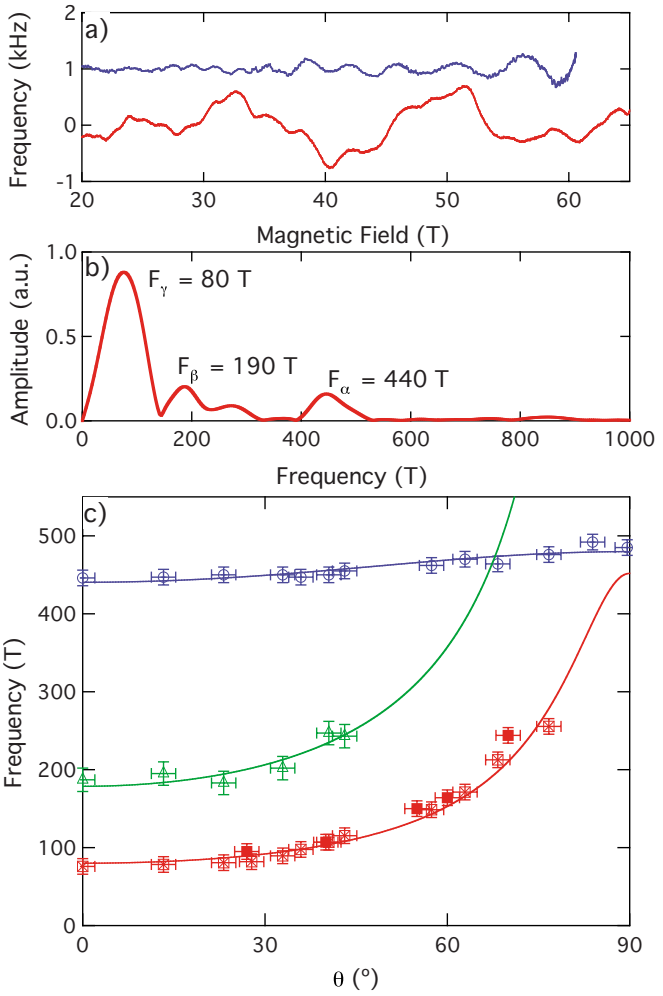

FIG. 2. (Color online) (a) The residual frequency shift of the TDO circuit (once a third order background has been subtracted) showing QOs periodic in inverse magnetic field. The upper curve is for the magnetic field oriented parallel to the c axis $\theta=0°$ and the lower curve for field perpendicular to the c axis. (b) The Fourier spectrum of the TDO data at $\theta=0°$. (c) The field orientation dependence of the QO frequencies. The hollow points are extracted form the TDO data the solid points are extracted from the torque data. The solid lines are fits to Fermi-surface volumes with an elliptical cross section oriented parallel to the c axis. The α, β, and γ frequencies correspond to a Fermi-surface cross section comprising $1.7\pm0.05\%$, $0.7\pm0.05\%$, and $0.30\pm0.02\%$ of the paramagnetic Brillouin zone. The ellipticity for α is $1.1\pm.1$, β is 5 ± 1, and γ is $5.6\pm.1$.

$=0.7\pm0.2m_e$ in sample B which are in broad agreement. The α pocket has a mass of $m^{*}_{\alpha}=1.2\pm0.3m_e$ and the β pocket has a mass of $m^{*}_{\beta}=0.6\pm0.3m_e$. The errors given in Fig. 2(c) are determined by the noise floor of the Fourier spectra. Furthermore we estimate the Dingle temperature for the pockets to be $T^{\alpha}_{D}=4$ K±1 and $T^{\gamma}_{D}=3$ K±1 though we are unable to extract this for the β pocket. The Dingle temperature was not accounted for in our effective-mass fitting.[14]

We next turn to the angle dependence of the observed pockets. Sample B was mounted on a probe that could be continuously rotated allowing us to collect a comprehensive data set on all frequencies. Sample A was discretely rotated and the QOs were only observable between ($27°<\theta<70°$) due to the loss in torque signal as the orientation of the field approaches a crystal-symmetry direction. Even in sample B the intensity of γ QOs is lost at angles $\theta>80°$ and β for $\theta>50°$. The γ and β pockets are highly eccentric, resembling elongated cigar shapes. By contrast, the α pocket has a very small angular dependence, suggesting that the pocket is much more isotropic and three dimensional. This frequency is likely not observable in the torque technique due to the smaller signal/noise or perhaps due to this absence of anisotropy. Finally, we find the orbitally averaged Fermi velocity for each pocket using the relation $v_F=\sqrt{2e\hbar F/m^*}$ yielding $v_{\gamma}=0.8\times10^5$ ms^{-1}, $v_{\beta}=1.3\times10^5$ ms^{-1}, and $v_{\alpha}=1.9\times10^5$ ms^{-1}.

The γ and β frequencies observed here do not correspond to any of the Fermi-surface pockets calculated for the nonmagnetic state of $BaFe_2As_2$.[15] The α pocket is comparable in size to a calculated pocket centered at Γ but the angle dependence reveals that the pocket is much more isotropic than that predicted in a nonmagnetic calculation. In agreement with the results in $SrFe_2As_2$ we conclude that a dramatic Fermi-surface reconstruction has occurred in this compound. The Fermi-surface pockets we observe are consistently larger than those in $SrFe_2As_2$, but the effective masses are smaller, keeping the orbitally average velocities about the same.[2] In order to gain further insight into our data we perform band-structure calculations including magnetic ordering which reconstruct the Fermi surface.[16] Our local-density approximation/generalized gradient approximation (LDA/GGA) calculations produce magnetic moments (1.67 and $1.97\mu_B$, respectively) that are higher than the experimentally measured moment of about $0.9\mu_B$ (Ref. 17) Because the Fermi surfaces have a dependence on the magnitude of the moment, we suppressed it to the experimental value using the well-known LDA+U methodology[18] but with a negative value for U. Whereas LDA+U with $U>0$ generally increases the magnetic tendencies of a system, the negative U has the opposite effect and with a value of $U=-0.54$, we achieve a calculated magnetic moment of $1.0\mu_B$. The band structure with and without this technique is shown in Fig. 3. To check the validity of our methodology, we also increased the magnitude of the negative U until the magnetic moment was suppressed entirely and then compared the band structure and Fermi surfaces to their nonspin-polarized counterparts. The agreement between Fermi surfaces was very good though shifts of more than 100 meV could be found elsewhere in the energy spectrum. Nonetheless, this partially suppressed moment calculation provides the best possible comparison to experiment. The results are summarized in Table I.

Four separate extremal orbits occur based on the calculated Fermi surfaces. These are labeled in Fig. 3 as 1 (hole), 2 (electron), 3 (hole), and 4 (electron). For the suppressed moment calculation, pocket 2 has an area consistent with the measured F_γ. The other calculated frequencies are either higher, 3 and 4, or much lower, 1, than any observed frequencies. However, it is common that calculations require an energy shift to achieve good agreement with experiment. The slightly oblate topology of 4 is inconsistent with the observed angle dependence of any of the pockets, so we believe it unlikely that this is associated with the present QOs. To find an orbit area similar to the α pocket we find that a upward shift in E_F of 60 meV would shrink pocket 3 to a similar size with an effective mass of $0.7m_e$, exhibiting a similar angle dependence to that observed. Both 1 and 2 have a topology consistent with the angle dependence of γ and β and the sharp pinching of the pockets at their extremities may explain the rapid loss of signal at large angles due to the phase smearing associated with a higher Fermi-surface curvature. Similarly if 2 is shifted upward by 33 meV it comes into agreement with the β orbit with an effective mass of $0.55m_e$. Finally 1 is shifted by 38 meV downward it comes into agreement with the γ orbit with an effective mass of $0.47m_e$. We thus settle on identifying γ with 1 β with 2 and

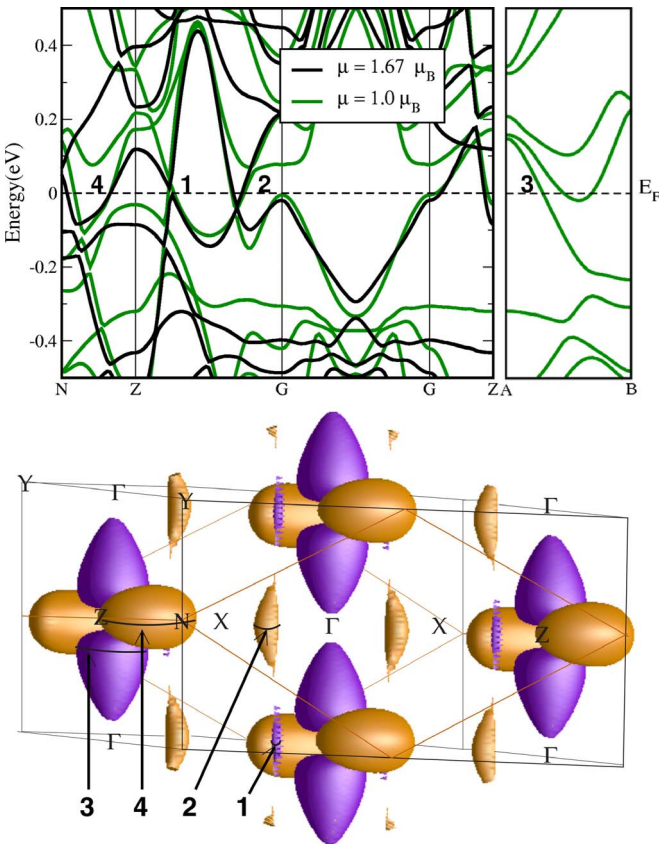

FIG. 3. (Color online) (Top) Band structure for the reconstructed state of $BaFe_2As_2$ calculated for a magnetic moment of $\mu=1.6$ (black) and $\mu=1.0$ (green/gray). Most of the pockets shown in Fig. 3 are made up of multiple bands. The Fermi surfaces of $BaFe_2As_2$ in the magnetic phase. (Bottom) High symmetry directions corresponding to the band structure of Fig. 3 are shown in black. The primitive Brillouin zone is shown in light (orange/light gray) nonorthogonal lines. Extremal orbits 1, 2, 3, and 4 for (001) magnetic field are indicated.

α with 3 which is the same identification scheme than the one used for $SrFe_2As_2$.[2] With our assignment, the effective mass of α is renormalized by a factor of 1.7, β by 1.1, and γ is renormalized by 2 compared to density functional theory (DFT). All of the shifts are well within the $\sim$100 meV error incurred in suppressing the magnetic moment to zero, though the margin of error is expected to be somewhat less for the smaller shift to $\mu=1.0\mu_b$.

The Sommerfeld coefficient has been extracted from heat capacity measured on these samples[11] and found to be $\gamma_S=6.1$ mJ/mol K^2, consistent with Ref. 19. The Sommerfeld coefficient calculated for the reconstructed Fermi surface is 2.83 mJ/mol K^2, as shown in Table I. This corresponds to a moderate renormalization of $\lambda=1.1$. This is consistent with the effective-mass renormalization necessary to reconcile our QOs with DFT, which implies that the present calculations account for the observed Fermi surface.

On the other hand, if we assume that the observed pockets occur only once in the Brillouin zone, we estimate a contribution of 1.73 mJ/mol K^2. It is possible that the large Fermi cylinders observed by a number of ARPES measurements, centered at the Γ point of the Brillouin zone[4,5,20–22] may ac-

TABLE I. Table of pocket size and effective mass expected to appear in magnetic QOs data, using a spin-polarized DFT calculation (described in text) for magnetic moment $\mu=1.6\mu_B$ and $\mu=1.0\mu_B$. The Sommerfeld coefficient γ_s expected for each calculation is also given. Bands from the $\mu=1.0$ calculation have been shifted by different amounts to match the observed pockets and the effective mass is recalculated.

	$\mu=1.6$ (Unshifted)		$\mu=1.0$ (Unshifted)		$\mu=1.0$ (Shifted)	
Orbit	%BZ	m_b/m_e	%BZ	m_b/m_e	%BZ	m_b/m_e
1	0.01		0.06	0.1	0.3	0.47
2	0.15	0.2	0.29	0.27	0.7	0.55
3	3.1	1.6	3.34	1.16	1.63	0.7
4	6.7	2.5	4.6	1.95		
γ_s		2.24		2.83		(mJ/mol K^2)

count for the remainder. However, given that each two-dimensional cylinder contributes ~ 1.5 mJ/mol K^2 per m_e, regardless of radius, the *maximum* effective mass available to each cylinder is $\sim 1.4m_e$, in contradiction to the ARPES results of Ref. 22. Furthermore, in order to reconcile the existence of the large pockets with the antiferromagentic ground state of $BaFe_2As_2$, an exotic nesting mechanism needs to be invoked.[21] In contrast, only small pockets are observed in the present measurements, consistent with DFT calculations for an antiferromagnetic ground state. This could arise due to conventional Fermi surface nesting, as in elemental Cr.

In summary, we have measured QOs in $BaFe_2As_2$ and found small pockets which are in broad agreement with band-structure calculations for an antiferromagnetic state. Our observations are consistent with a conventional spin-density wave picture which folds the bands of the nonmagnetic state.

The authors would like to thank Nigel Hussey, Antony Carrington, and Igor Mazin for useful comments on this work before publication. This work is supported by the Department of Energy, Office of Basic Energy Sciences under Contract No. DE-AC02–76SF00515 and partly funded by EPSRC under Grant No. EP/F038836/1. Work performed at the NHMFL was primarily funded by NSF and the state of Florida.

[1] A. I. Coldea, J. D. Fletcher, A. Carrington, J. G. Analytis, A. F. Bangura, J.-H. Chu, A. S. Erickson, I. R. Fisher, N. E. Hussey, and R. D. McDonald, Phys. Rev. Lett. **101**, 216402 (2008).

[2] Suchitra E. Sebastian, J. Gillett, N. Harrison, P. H. C. Lau, D. J. Singh, C. H. Mielke, and G. G. Lonzarich, J. Phys.: Condens. Matter **20**, 422203 (2008).

[3] F. Pfuner, J. G. Analytis, J.-H. Chu, I. R. Fisher, and L. Degiorgi, Eur. Phys. J. B **67**, 513 (2009).

[4] D. Hsieh, Y. Xia, L. Wray, D. Qian, K. Gomes, A. Yazdani, G. F. Chen, J. L. Luo, N. L. Wang, and M. Z. Hasan, arXiv:0812.2289 (unpublished).

[5] L. X. Yang, Y. Zhang, H. W. Ou, J. F. Zhao, D. W. Shen, B. Zhou, J. Wei, F. Chen, M. Xu, C. He, Y. Chen, Z. D. Wang, X. F. Wang, T. Wu, G. Wu, X. H. Chen, M. Arita, K. Shimada, M. Taniguchi, Z. Y. Lu, T. Xiang, and D. L. Feng, Phys. Rev. Lett. **102**, 107002 (2009).

[6] Jun Zhao, Q. Huang, Clarina de la Cruz, Shiliang Li, J. W. Lynn, Y. Chen, M. A. Green, G. F. Chen, G. Li, Z. Li, J. L. Luo, N. L. Wang, and Pengcheng Dai, Nat. Mater. **7**, 953 (2008).

[7] R. A. Ewings, T. G. Perring, R. I. Bewley, T. Guidi, M. J. Pitcher, D. R. Parker, S. J. Clarke, and A. T. Boothroyd, Phys. Rev. B **78**, 220501(R) (2008).

[8] J. Zhao, D.-X. Yao, S. Li, T. Hong, Y. Chen, S. Chang, W. Ratcliff, J. W. Lynn, H. A. Mook, G. F. Chen, J. L. Luo, N. L. Wang, E. W. Carlson, Jiangping Hu, and Pengcheng Dai, Phys. Rev. Lett. **101**, 167203 (2008).

[9] I. I. Mazin and M. D. Johannes, Nat. Phys. **5**, 141 (2009).

[10] Y. Ran, F. Wang, H. Zhai, A. Vishwanath, and D.-H. Lee, Phys. Rev. B **79**, 014505 (2009).

[11] J.-H. Chu, J. G. Analytis, C. Kucharczyk, and I. R. Fisher, Phys. Rev. B **79**, 014506 (2009).

[12] A. S. Sefat, R. Jin, M. A. McGuire, B. C. Sales, D. J. Singh, and D. Mandrus, Phys. Rev. Lett. **101**, 117004 (2008).

[13] D. Shoenberg, *Magnetic Oscillations in Metals*, 1st ed. (Cambridge University Press, Cambridge, 1984).

[14] The observation of multiple orbits and the experimental signal/noise necessitates performing the Fourier analysis for extracting m^* over a relatively wide range of $B=20-60$ T. This combined with the large Dingle temperatures we observe is known to lead to a systematic underestimate of m^*. We estimate this to be $<20\%$ for both m^*_α and m^*_γ.

[15] D. J. Singh, Phys. Rev. B **78**, 094511 (2008).

[16] Calculations were performed using an augmented plane wave plus local-orbital (APW+lo) code, WIEN2K (Ref. 23). For the results presented in this work, we used the experimental lattice coordinates and ionic positions and the LDA (Ref. 24) to the exchange-correlation potential. We included the spin-orbit interaction in both LDA and the GGA and the latter produces a higher magnetic moment, the electronic structure is sensitive to the magnitude of the moment and this, in turn, is very sensitive to the structure, specifically the height of the As atom above the Fe atom.

[17] Q. Huang, Y. Qiu, W. Bao, M. A. Green, J. W. Lynn, Y. C. Gasparovic, T. Wu, G. Wu, and X. H. Chen, Phys. Rev. Lett.

101, 257003 (2008).

[18] V. I. Anisimov and O. Gunnarsson, Phys. Rev. B **43**, 7570 (1991); A. G. Petukhov, I. I. Mazin, L. Chioncel, and A. I. Lichtenstein, *ibid.* **67**, 153106 (2003).

[19] J. K. Dong, L. Ding, H. Wang, X. F. Wang, T. Wu, G. Wu, X. H. Chen, and S. Y. Li, New J. Phys. **10**, 123031 (2008).

[20] Y. Zhang, J. Wei, H. W. Ou, J. F. Zhao, B. Zhou, F. Chen, M. Xu, C. He, G. Wu, H. Chen, M. Arita, K. Shimada, H. Namatame, M. Taniguchi, X. H. Chen, and D. L. Feng, Phys. Rev. Lett. **102**, 127003 (2009).

[21] V. B. Zabolotnyy, D. V. Evtushinsky, A. A. Kordyuk, D. S. Inosov, A. Koitzsch, A. V. Boris, G. L. Sun, C. T. Lin, M. Knupfer, B. Buechner, A. Varykhalov, R. Follath, and S. V. Borisenko, Nature (London) **457**, 569 (2009).

[22] H. Ding, K. Nakayama, P. Richard, S. Souma, T. Sato, T. Takahashi, M. Neupane, Y.-M. Xu, Z.-H. Pan, A. V. Federov, Z. Wang, X. Dai, Z. Fang, G. F. Chen, J. L. Luo, and N. L. Wang, arXiv:0812.0534 (unpublished).

[23] P. Blaha, K. Schwarz, G. K. H. Madsen, D. Kvasnicka, and J. Luitz, WIEN2K, An augmented planewave+local orbitals program for calculating crystal properties (Technische Universitat Wien, 2002, Austria); http://www.wien2k.at

[24] J. P. Perdew and Y. Wang, Phys. Rev. B **45**, 13244 (1992).